Label-Free Efficient and Accurate Detection of Cystic Fibrosis Causing Mutations Using an Azimuthally Rotated GC-SPR Platform

ARTICLE *in* ANALYTICAL CHEMISTRY · OCTOBER 2014

Impact Factor: 5.64 · DOI: 10.1021/ac503272y · Source: PubMed

7 AUTHORS, INCLUDING:

Agnese Antognoli
Veneto Nanotech
19 PUBLICATIONS **185** CITATIONS
SEE PROFILE

Gabriele Zacco
Veneto Nanotech
26 PUBLICATIONS **110** CITATIONS
SEE PROFILE

Gianluca Ruffato
University of Padova
36 PUBLICATIONS **172** CITATIONS
SEE PROFILE

Filippo Romanato
University of Padova
217 PUBLICATIONS **2,171** CITATIONS
SEE PROFILE

analytical chemistry

Article

pubs.acs.org/ac

Label-Free Efficient and Accurate Detection of Cystic Fibrosis Causing Mutations Using an Azimuthally Rotated GC-SPR Platform

Anna Meneghello,[†,‡,#] Agnese Antognoli,[†] Agnese Sonato,[*,§,∥,⊥,#] Gabriele Zacco,[§,⊥] Gianluca Ruffato,[∥,⊥] Erica Cretaio,[†] and Filippo Romanato[§,∥,⊥]

[†]Veneto Nanotech S.C.p.A., Via S. Crispino 106, Padova, Italy, c/o Nanofab, Via delle Industrie 5, 30175 Marghera (VE), Italy

[‡]University of Padova, Department of Biology, viale G. Colombo, 3 - via U. Bassi, 58/B, 35131 Padova, Italy

[§]IOM-CNR, Area Science Park, S.S. 14 km 163.5, 34149 Basovizza (TS), Italy

[∥]University of Padova, Department of Physics, Via F. Marzolo 8, 35131 Padova, Italy

[⊥]Veneto Nanotech S.C.p.A., Via S. Crispino 106, Padova, Italy, c/o LaNN - Laboratory for Nanofabrication of Nanodevices, Corso Stati Uniti 4, 35127 Padova, Italy

ABSTRACT: Plasmonic nanosensors are candidates for the development of new sensors with low detection limits, high sensitivity, and specificity for target detection: these characteristics are of critical importance in the screening of mutations responsible for inherited diseases. In this work, we focused our study on the detection of some of the most frequent mutations responsible for cystic fibrosis (CF) among the Italian population. For the detection of the CF mutations we adopted a recently developed and highly sensitive Grating Coupled−Surface Plasmon Resonance (GC-SPR) enhanced spectroscopy method for label-free molecular identification exploiting a conical illumination configuration. Gold sinusoidal gratings functionalized with heterobifunctional PEG were used as sensing surfaces, and the specific biodetection was achieved through the coupling with DNA hairpin probes designed for single nucleotide discrimination. Such substrates were used to test unlabeled PCR amplified homozygous wild type (wt) and heterozygous samples, deriving from clinical samples, for the screened mutations. Hybridization conditions were optimized to obtain the maximum discrimination ratio (DR) between the homozygous wild type and the heterozygous samples. SPR signals obtained from hybridizing wild type and heterozygous samples show DRs able to identify univocally the correct genotypes, as confirmed by fluorescence microarray experiments run in parallel. Furthermore, SPR genotyping was not impaired in samples containing unrelated DNA, allowing the platform to be used for the concomitant discrimination of several alleles also scalable for a high throughput screening setting.

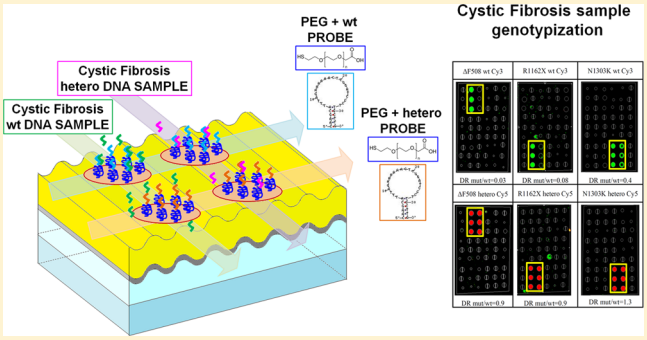

Cystic fibrosis (CF) is one of the most common life-shortening inherited diseases among the Caucasian population, as its incidence is 1 in 2000−2500 live births. CF, inherited in a Mendelian autosomal recessive way, is caused by mutations in the cystic fibrosis transmembrane conductance regulator (CFTR) gene, identified in 1989[1] and coding for a chlorine ion channel protein.[2−4] An abnormal CFTR protein results in defective electrolyte transport and defective chloride ion transport in the apical membrane epithelial cells of the sweat gland, airway, pancreas, and intestine.

As recessive diseases, CF presents "carrier" individuals: these are genetically heterozygous for a specific mutation on CFTR gene, i.e. only one of the two CTFR alleles carries the mutation (wild type/mutant alleles: wt/mut). Heterozygotes are phenotypically normal, as healthy as individuals with both wild type alleles (wild type/wild type alleles: wt/wt), defined as wt homozygous.

When a particular mutation is instead present on both alleles of the CFTR gene, a mut homozygous condition is recognized, and individuals with this genetic profile are phenotypically affected by CF disease.

Almost 1000 different mutations have been identified in the CF gene, however, the vast majority of them are at frequencies lower than 0.1%. The most frequent mutation, ΔF508, accounts for 30%−88% of CF chromosomes worldwide, depending upon race/ethnicity. Among the Italian population, ΔF508 has a frequency in carriers of more than 40%, followed by two other mutations with a frequency in carriers of 5−6% each: R1162X and N1303K.[5,6] CF genotyping has seen rapid and efficient growth in recent years since, more than the most commonly used CF diagnostic techniques, novel assays and methods might be employed to enhance the detection throughput performances. The most widely traditional used

Received: September 1, 2014
Accepted: October 31, 2014

   dx.doi.org/10.1021/ac503272y | *Anal. Chem.* XXXX, XXX, XXX−XXX

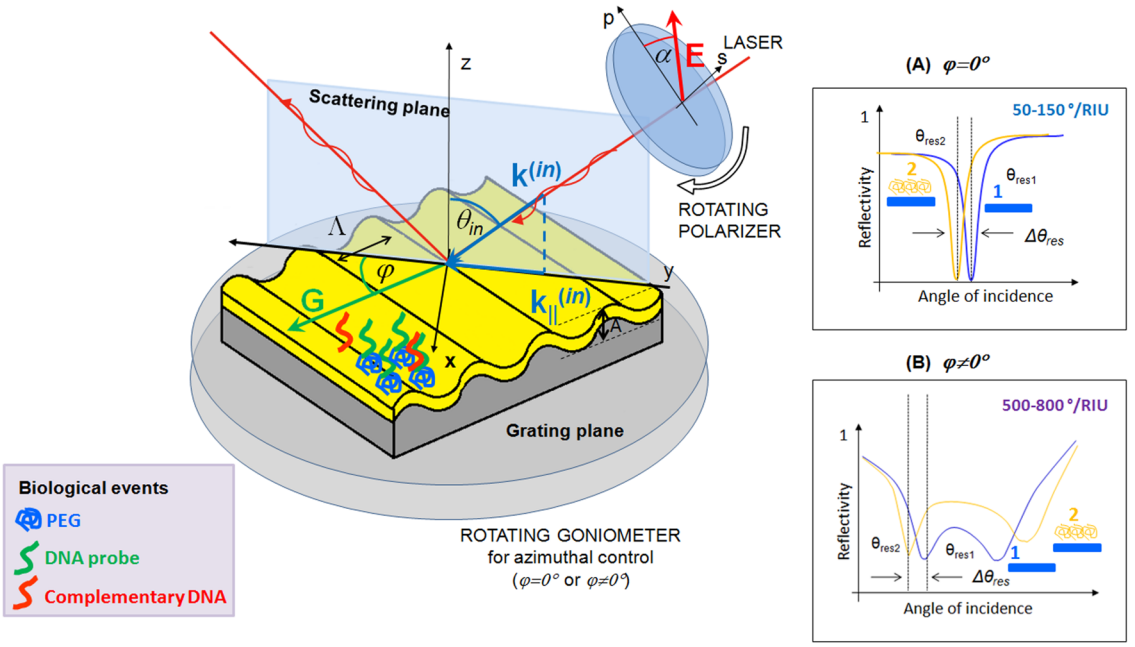

Figure 1. Scheme of the experimental configuration geometry from Ruffato and Romanato.[37] The plasmonic substrate (period Λ = 500 nm and amplitude A = 40 nm) is mounted onto a rotating goniometer allowing the azimuthal control of the grating plane. In the azimuthal rotated configuration ($\varphi \neq 0°$), the photon scattering plane is rotated by an angle φ with respect to the grating vector **G**, so that when the coupling between the incident photon momentum ($\mathbf{k}^{(in)}$) and the surface plasmon polariton momentum occurs for a certain incident wavelength (λ_{in}) and angle (θ_{in}), a double reflectivity dip is registered, and sensitivities range from 500 to 800°/RIU (inset B). In the null azimuth configuration ($\varphi = 0°$), a single reflectivity dip is registered, and sensitivities range from 50 to 150°/RIU (inset A). Light polarization could be tuned through a rotating polarizer (α is the polarization angle). Biological events on a surface are detected by the resonance angle shift ($\Delta\theta_{res}$) derived from the reflectivity spectra.

techniques to diagnose CF are ASO dot-blot, based upon hybridization of a labeled oligonucleotide probe with the target DNA anchored to a membrane, and reverse dot-blot, in which oligonucleotide probes are bound to the membrane on which the biotinylated amplified target DNA is hybridized.[7−10] Other detection techniques based on nucleic acid specific amplification and identification include Amplification Refractory Mutation System (ARMS) or allele specific amplification,[11,12] oligoligation assay (OLA),[13,14] polyacrylamide gel electrophoresis (PAGE) separation of the heteroduplexes,[15] single-stranded conformation polymorphism (SSCP),[16,17] and denaturing gradient gel electrophoresis (DGGE).[18]

More recently, biosensor-based techniques for the detection of CF mutation were reported, as electrochemical biosensors based on methylene blue-DNA interaction,[19] DNA microarrays,[20−25] or biospecific interaction analysis (BIA) monitored through Surface Plasmon Resonance (SPR) based technology,[26−31] performed both through the usage of DNA and PNA molecules.[32,33]

SPR is a promising high-sensitivity, fast, and low cost technique that meets the requirements for the development of reliable accurate methods in the detection of CF mutations. Most of the literature results based on the SPR technique are performed using the prism-coupling detection method (PC-SPR) and synthetic complementary oligonucleotides as target DNA, and limited evidence is available assessing the performances of SPR-based biosensors on clinical samples. Typically, in these studies, a single mutation is analyzed at a time, to discriminate between homozygous and heterozygous states, e.g. in CFTR,[26,27,30] in BRCA1,[34] or in p53 gene.[35]

In the present work, we focused our study on the development of a DNA/DNA azimuthally rotated grating-coupled surface plasmon resonance (GC-SPR)-based sensor[36] for the detection of some of the most common CFTR related mutations. GC-SPR under azimuthal control, as demonstrated in its first application in simple chemical systems,[36,37] gives the possibility to enhance the SPR detection sensitivity up to 1 order of magnitude (up to 600 and 800°/RIU) with respect to standard GC- and PC-SPR methods (typically 50−150°/RIU).[38] In addition, more SPPs can be supported with the same illuminating wavelength. On top of that, through symmetry breaking after grating rotation, polarization assumes a fundamental role on surface plasmon polaritons excitation, and it must be properly tuned in order to optimize the coupling strength. In Figure 1, the scheme of GC-SPR configuration under azimuthal control is depicted. Recently, the possibility of applying the azimuthally rotated GC-SPR technique to a wide range of sensing configurations was demonstrated in the case of avidin−biotin interaction and DNA-PNA hybridization.[38,39]

Allele specific oligonucleotide (ASO) stem-loop probes have been designed to achieve precise CF genotyping due to the presence of a hairpin forming region. In the presence of a full complementary DNA, the probe loses its closed structure, allowing the formation of a stable hybrid, while in the presence of mismatched or noncomplementary DNA it maintains its secondary structure.[40,41]

Clinical PCR amplified samples—derived both from homozygous wild type (wt/wt) and clinical heterozygous samples (wt/mut)—were used to set up the SPR system, and results were compared also to fluorescent-based microarray experiments in terms of genotyping ability and discrimination power. Experiments were also performed using PCR amplified samples mixed with fragmented human genomic DNA as an interferent to verify the efficacy of the detection performances of the SPR sensor.

dx.doi.org/10.1021/ac503272y | Anal. Chem. XXXX, XXX, XXX−XXX

Table 1. PCR Primers for CFTR Genomic Regions' Amplification[a]

name	sequence 5′-3′	nt	GC%	amplicon length (wt/mut)	melting temperature (T_m °C)
ΔF508 (ex10) F	ATGATGGGTTTTATTTCCAGAC	22	36.4	271/268	50.9
ΔF508 (ex10) R	ATTGGGTAGTGTGAAGGGTTC	21	47.6		54.6
R1162X (ex19) F	GCCCGACAAATAACCAAGTGA	21	47.6	454/454	55.5
R1162X (ex19) R	GCTAACACATTGCTTCAGGCT	21	47.6		55.8
N1303K (ex21) F	AATGTTCACAAGGGACTCCA	20	45.0	473/473	53.9
N1303K (ex21) R	CAAAAGTACCTGTTGCTCCA	20	45.0		52.9

[a]Primer sequences were adapted from sequences reported by Zielenski et al.[42] nt: nucleotide length. GC%: guanine-cytosine percentage. wt: wild type DNA. mut: mutant DNA.

These results successfully proved the reliability of the SPR platform in discriminating between the presence of a wild type or mutant allele in the samples.

EXPERIMENTAL SECTION

Chemicals and Solutions. All the reagents and solution components used were purchased from Sigma-Aldrich (St. Louis, MO, USA), if not otherwise specified.

Used solutions and buffers have the following composition: Basic piranha solution: 5:1:1 dd-H_2O, 30% H_2O_2 and 30% NH_4OH. MES buffer for −COOH activation: 0.1 M 2-(N-morpholino) ethanesulfonic acid (MES), 0.5 M NaCl, pH 6.0. Saline-sodium citrate (SSC) buffer 20X: 3 M sodium chloride, 300 mM trisodium citrate, pH 7.0. Microarray printing buffer 6X: 300 mM sodium phosphate, 0.02% Triton, pH 8.5. Microarray blocking solution: 0.1 M Tris, 50 mM ethanolamine, pH 9. Microarray washing solution: 4X SSC, 0.1% sodium sodecyl sulfate (SDS). The water used was of bidistilled (dd-H_2O) or Milli-Q grade.

The sensing platforms were fabricated by combining laser interference lithography (LIL) at TASC-IOM-CNR laboratories (Basovizza, TS, Italy) and soft lithography techniques were performed at LaNN laboratories (Veneto Nanotech s.c.p.a., Padova). S1805 photoresist was purchased from Microposit (Shipley European Limited, UK), while MF319 Developer and PGMEA (propylene glycol monomethyl ether acetate) were purchased from MicroChem Corp (Newton, MA, USA). PDMS (polydimethylsiloxane; Sylgard 184) was purchased from Dow-Corning Corp. (Midland, MI, USA), and the thiolene resin, used for the lithographic master replica, NOA 61 (Norland Optical Adhesive). was purchased from Norland Products Inc. (Las Vegas, NV, USA).

Allele Specific Oligonucleotide DNA Probes Design. The three most frequent mutations among the Italian population of the CFTR gene were selected (ΔF508, R1162X, N1303K), and their localization was verified through the CFTR mutation database (http://www.genet.sickkids.on.ca/app). For each mutation, a pair of primers able to amplify the genomic portion of interest through PCR was selected (Table 1). Based on the genomic regions identified by the relative primers, specific wild type (wt) and mutant (mut) probes for DNA microarrays were selected, using Array Designer software (Premier Biosoft, CA, USA).

According to literature's information, a length of 18−22 nucleotides was chosen as optimal for probes' design, to discriminate single base mutations with high accuracy. It should be noted that the probes' design was highly constrained by the position of the mutation itself, which should be placed in the central position of the probe, in order to maximize mutation discrimination capability,[43,44] and by the nucleotide composition of the sequence surrounding the mutation itself. Selected probes were also checked for their specificity through the Basic Local Alignment Search Tool (BLAST).

For the complete ASO probe design, a portion of each hairpin was defined with a length of six base pairs. We examined the stability of the secondary structure in order to standardize the T_m and ΔG of the hairpin region of all the created structures. Results obtained for the hairpin selected portions and for the final probes are summarized in Table 2. The hairpin portion is indicated in bold and underlined; probes with the hairpin portion show excellent uniformity in chemical−physical characteristics, especially concerning the average T_m. Probes were purchased from IDT Integrated DNA Technologies (Leuven, Belgium) with a 5′ C6-NH_2 modification, to allow subsequent surface functionalization.

SPR Substrate Fabrication and Characterization. The sinusoidal grating fabrication process is summarized in the following steps. (1) *Laser interference lithography (LIL).* A S1805/PGMEA solution (2:3) was spun onto a silicon wafer with a spin speed of 6000 rpm for 30 s. The sample was exposed to a 50 mW helium cadmium (HeCd) laser emitting a TEM00 single mode at a 325 nm light source with a beam incidence angle of 19° and an exposure dose of 70 mJ/cm^2. Resist developing was performed by immersing the samples in a MF319/Milli-Q water (10:1) solution for 15 s. The exposure and process parameters (i.e., beam incidence angle, exposure, and developing time) were chosen in order to obtain a sinusoidal grating with a period of 500 nm and a peak-to-valley amplitude of 40. (2) *Soft lithography.* For the replica of the just prepared nanostructure, a PDMS mold was realized curing the PDMS layer dropped onto the resist grating at 60 °C for 4 h. The nanopattern was imprinted onto a thiolene resin film (NOA 61) supported onto a microscope glass slide, illuminating the PDMS mold with ultraviolet (UV) light (λ = 365 nm) for 30 s, using a standard metal halide 50 mW/cm^2 lamp (DYMAX UV light flood lamp curing system). The final plasmonic substrate consisted of two identical gratings imprinted onto a microscope glass slide of 75 mm × 25 mm. (3) *Thermal evaporation.* A gold (40 nm) layer was evaporated above the patterned resin film and a thin chromium film (5 nm) was used as adhesion layer between the metal and the underlying dielectric medium.

A VEECO D3100 Nanoscope IV atomic force microscope (AFM) and a dual beam FEI Nova 600i scanning electron microscope were adopted to characterize the substrate topography and sinusoidal profile (Figure 3).

SPR Surface Dressing and Functionalization. Substrates were preliminarily cleaned with a basic piranha solution for 10 min, rinsed, and dried under a nitrogen flux. A heterobifunctional thiol-PEG (poly(ethylene glycol) 2-mercaptoethyl ether acetic acid, M_w 3.4 kDa, SH-PEG-COOH) was used to functionalize the surface, upon an incubation of 24 h in a humidified

dx.doi.org/10.1021/ac503272y | Anal. Chem. XXXX, XXX, XXX−XXX

Table 2. Sequence of Microarray ASO Probes[a]

Name	Sequence 5'-3'	Structure	nt	Tm °C	GC%	ΔG hairpin portion kcal/mol	Tm hairpin portion °C	ΔH hairpin portion kcal/mol	ΔS hairpin portion kcal/mol
ΔF508	**CAATCG**AATATC ATCTTTGGTGTT TCCT**CGATTG**	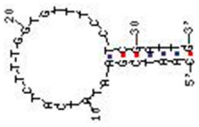	34	59,2	38,2	-3,2	44,7	-51,5	-162,02
ΔF508 mut	**CAATCG**ATATCA TTGGTGTTTCCT ATG**TCGATTG**	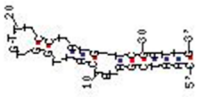	34	59,0	38,2	-4,87	43,6	-83	-262,07
R1162X	**CCATCA**TCTGTG AGCCGAGTCTTT **TGATGG**	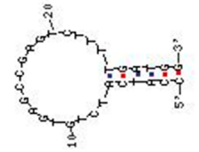	30	62,1	50,0	-2,24	41,5	-42,8	-136,02
R1162X mut	**CCATCA**ATCTGT GAGCTGAGTCTT TA**TGATGG**	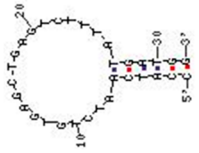	32	60,1	43,8	-2,47	42,9	-43,6	-137,96
N1303K	**CAAGCA**TTTAGA AAAAACTTGGAT CCCT**TGCTTG**	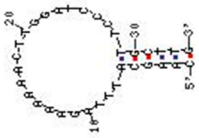	34	60,2	38,2	-2,52	42,7	-44,9	-142,15
N1303K mut	**CAAGCA**TTTAGA AAAAAGTTGGAT CCCT**TGCTTG**	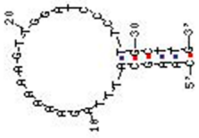	34	60,2	38,2	-2,52	42,7	-44,9	-142,15

[a]The hairpin region with the mutated oligonucleotides is represented in red, and the hairpin portion is bold and underlined. Thermodynamic analysis was performed using IDT DNA software (http://eu.idtdna.com/analyzer/applications/oligoanalyzer/), evaluating with software default parameters (oligo concentration = 0.25 μM, Na^+ concentration = 50 mM) the whole probe sequence and the hairpin structure (T = 25 °C, Na^+ concentration = 25 mM, suboptimality = 50%).

environment. Amino modified CFTR probes were covalently bound to the −COOH surface groups, previous EDC (N-(3-(dimethylamino)propyl)-N′-ethylcarbodiimide hydrochloride) −S-NHS (*N*-hydroxysulfosuccinimide sodium salt) activation in a MES buffer for 15 min. Gratings were functionalized with the usage of a ProPlate 64 slide chamber multiwells (Sigma-Aldrich), and up to 16 wells of 3.5 mm × 3.5 mm were obtained for each grating. Each well was functionalized with a single specific probe, leaving two empty cells per grating as measurement references.

Microarray Surface Functionalization. For fluorescent experiments, microarray deposition was performed on e-surf LifeLine slides (25 mm × 75 mm, LifeLineLab, Pomezia, Italy). Surfaces were printed by VersArray Chip Writer Pro System (Biorad, Hercules, CA), using Telechem SMP3 microspotting pins (Arrayit Corporation, Sunnyvale, CA). Amino-modified probes, diluted in Microarray Printing Buffer 1.5×, were printed to a final concentration of 20 μM. In a single microarray slide, up to 48 subarrays were printed; six replicas of alignment probes were spotted, plus three replicas of each investigated wt or mut probe, to ensure proper statistical analysis (Figure 2). Printed slides were incubated overnight in a 75% humidity incubation chamber, blocked, and washed according to standard protocols as specified by the supplier with microarray blocking and washing solutions, respectively, then ready for subsequent hybridization.

dx.doi.org/10.1021/ac503272y | *Anal. Chem.* XXXX, XXX, XXX−XXX

AL	10W	10M	B	B	AL
AL	10W	10M	B	B	AL
AL	10W	10M	B	B	AL
V	V	V	V	V	B
V	V	V	V	V	B
V	V	V	V	V	B
V	19W	19M	21W	21M	V
V	19W	19M	21W	21M	V
V	19W	19M	21W	21M	V

Figure 2. Deposition scheme of each of the 48 subarrays adopted for microarray printing on e-surf LifeLine slides. V = empty spots, B = buffer, AL = alignment spots. 10W, ΔF508 wt probe; 10M, ΔF508 mut probe; 19W, R1162X wt probe; 19M, R1162X mut probe; 21W, N1303K wt probe; 21M, N1303K mut probe.

Samples Preparation and Hybridization. DNA extracts were kindly provided by Dr. L. Picci (Pediatric Department, Padua Hospital, University of Padua). In particular, a homozygous wild type (wt/wt alleles) and a heterozygous (wt/mut alleles) sample for each of the three analyzed mutations were obtained after verification through DNA sequencing. No homozygous mutant samples were available.

DNA samples were PCR amplified using AmpliTaq Gold 360 DNA polymerase reagents (Applied Biosystem, Life Technologies, Milan, Italy).

PCR products were purified with silica spin columns (PureLink PCR Purification Kit, Life Technologies) and analyzed through an electrophoretic run on an Agilent Bioanalyzer with a DNA chip (Agilent Technologies, Santa Clara, CA). Fluorescent PCR products were obtained using a mix of dCTP-Cy3 or dCTP-Cy5, for wt or heterozygous samples, respectively (GE Healthcare, Little Chalfont, UK). Fluorophore incorporation was verified spectrophotometrically (NanoPhotometer, Implen, München, Germany).

The human genome from the lymphoma cell line (BL41 cell line, LGC standards, UK) was extracted with QIAamp DNA Mini Kit (Qiagen, Hilden, Germany) and fragmented with double strand DNA Fragmentase under the conditions indicated by the supplier (New England Biolabs, Ipswich, MA, USA). Obtained fragments ranged from 300 bp to 600 bp, as verified by capillary gel electrophoresis with the Agilent Bioanalyzer, and were used as interferent DNA in the subsequent preparations.

CFTR PCR fragments, Cy3/Cy5-labeled or unlabeled, were incubated on e-surf microarray slides and on gold plasmonic slides, respectively. Mixtures were denatured, cooled, and hybridized for 3 h at 37 °C, in a hybridization buffer (2X SSC, 0.1% SDS, 0.2 mg/mL Bovine Serum Albumin, 20% formamide), in the Array Booster AB410 hybridization station (Advalytix, Munich, Germany). ProPlate 64 multiwells slide chambers were used to physically isolate each subarray during incubation with different samples. For fluorescent analysis, one PCR sample can be simultaneously tested for the mutation of interest in the whole subarray that includes the six specific probes (three wild type and three mutants, each in triplicate, see Figure 2). For SPR experiments, instead, each PCR product obtained for all of the three loci needed to be split into two wells to analyze separately the wild type and the mutated allele of a single mutation at the same time.

After hybridization, slides were washed in the Advawash Station AW400 (Advalytix) for 5 min in 1X SSC 0.1% SDS at 37 °C, 2 min in 0.2X SSC, 2 min in 0.1X SSC and 30 s in dd-H_2O, spin-dried using Microarray High-Speed Centrifuge (Arrayit Corporation, Sunnyvale, CA) and submitted to SPR analysis or scanned for fluorescent emission.

SPR Measurements. A J.A. Woollam Co. VASE ellipsometer with angular and wavelength spectroscopic resolution of 0.005° and 0.3 nm, respectively, was used for the reflectivity measurements on the SPR surface. A goniometer with a precision of 5′ mounted onto the sample holder allowed the sample azimuthal orientation control. For the null azimuth detection, the incident wavelength (λ) was set to 725 nm, while for the rotated azimuth, one λ was set to 625 nm, the azimuthal angle (φ) to 45°, and the incident light polarization (α) to the value of 140° in order to optimize dip depth (α = 0° corresponds to TM polarization). In the azimuthally rotated GC-SPR, in fact, TM polarization is no longer the optimal one for SPP coupling, and the polarization angle should be tuned according to the formula $\tan \alpha = -\tan \varphi \cos \theta$, θ being the resonance polar angle.[45] In both cases, incident angles ranged from 20° to 80° by a step of 0.2°.

Each surface was characterized before dressing procedures and after each functionalization step. For each well, the analysis time required was 1 min per step. For each sample, two replicas were performed on each grating, and four replicas were therefore available in a single slide, composed by two gratings.

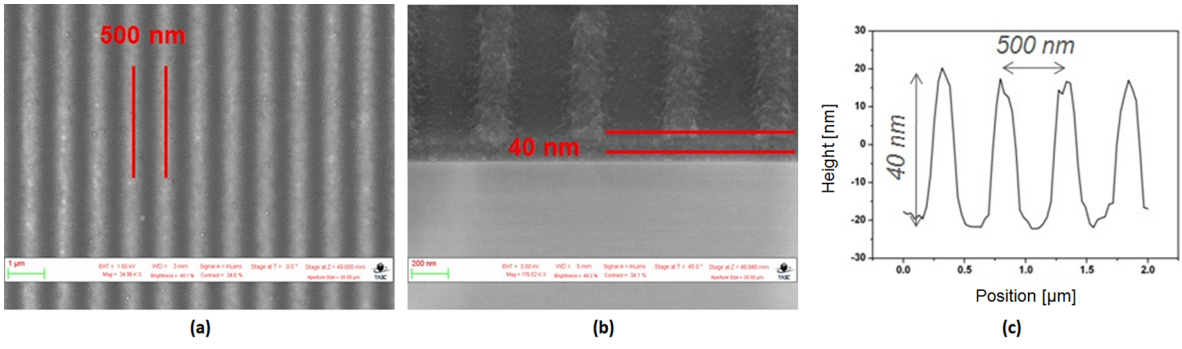

Figure 3. Surface topography SEM images (a, b) of the sinusoidal plasmonic substrate realized in this work. The sinusoidal profile was collected by AFM measurements (c).

dx.doi.org/10.1021/ac503272y | Anal. Chem. XXXX, XXX, XXX−XXX

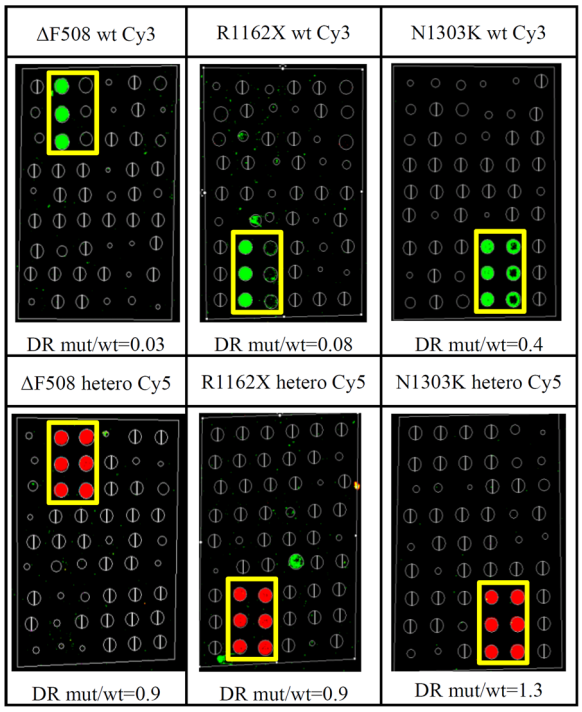

Figure 4. Microarray hybridization results obtained with PCR fragments, labeled with Cy3 (green, homozygous wt samples) or with Cy5 (red, heterozygous samples) under the optimized hybridization conditions (SSC2X, formamide 20%, hybridization temperature 37 °C 3h). Results are shown both as images and numerically as discrimination ratios (DR). Yellow boxes: include wt and mut probe for the analyzed mutation. wt: wild type samples. hetero: heterozygous samples.

Fluorescent Measurements. Fluorescent measurements on hybridized array were performed using a Genepix 4000B laser scanner (Molecular Devices, Sunnyvale, CA) and the Gene Pix Pro software using both 532 and 635 nm wavelengths. Fluorescent spot intensities were quantified using the Gene Pix Pro software after normalizing the data by subtracting local background from the recorded spot intensities. For each samples, five replicas were performed, each of them consisting in a subarray with a set of triplicate probes for each analyzed mutation.

RESULTS AND DISCUSSION

Plasmonic Sinusoidal Substrate Surface. Characterization of grating surfaces post fabrication is reported in Figure 3. For quality control, AFM and SEM images are recorded of the sinusoidal gratings used as sensing substrates in the genotyping experiments. Typically, gratings have a period of 500 nm and peak-to-valley amplitude of 40 nm.

Hybridization Conditions Setup and Optimization through Fluorescent Analysis. Hybridization conditions for the CFTR microarray were first set up through the preliminary usage of complementary fluorescent (Cy3 and Cy5) oligonucleotides. The performances of the chosen hybridization setting were subsequently confirmed using fluorescently labeled PCR products deriving from clinical samples to analyze the screening potential of the platform. Several conditions were deeply investigated, applying variations to SSC and formamide concentrations and to hybridization temperature to achieve optimal genotypization.

The hybridization protocol that allowed detecting the proper allele with the higher specificity included a buffer composition

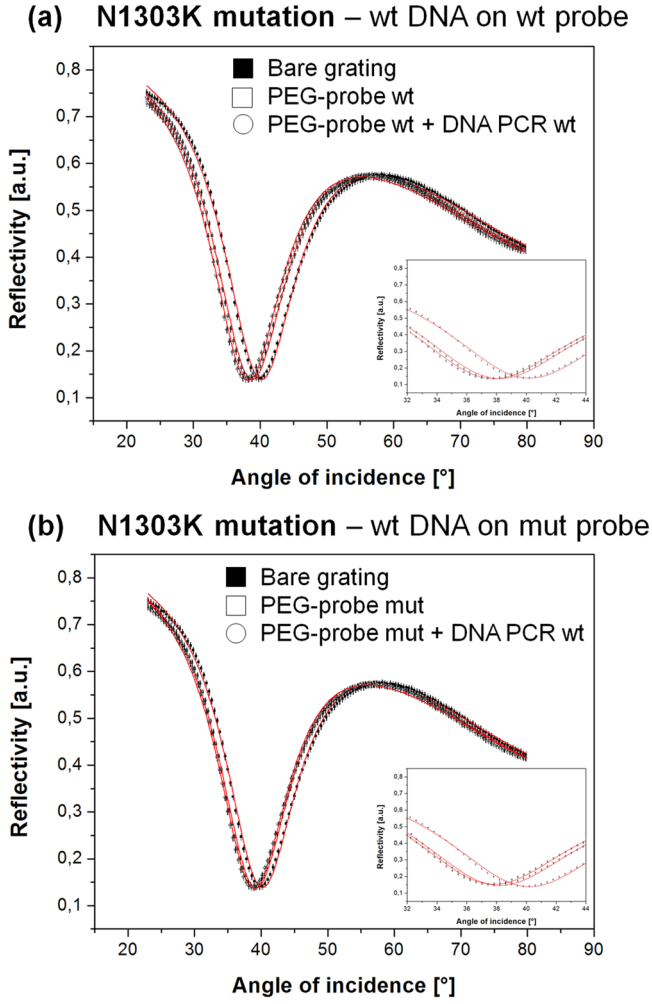

Figure 5. SPR shifts obtained after hybridization of CFTR related PCR products for N1303K allele. The sample was incubated both on wt and on mut related probes, and only the case of homozygous wt sample is reported as an example: wt sample onto wt probe (a) and wt sample onto mut probe (b). In the main figure, the reflectivity curves collected for the bare grating after substrate cleaning (full squares), after SH-PEG-COOH plus NH2 modified probe immobilization on the surface (empty squares), and after sample incubation empty circles) are shown. Three measurements per point were performed. The curves were fitted using a Lorentz function (red line), and the error was propagated and then mediated on all the measurements. The reflectivity minimum, clearly visible in the inset, was derived from the fitting procedure. For all the obtained graphs, the full width at half-maximum (fwhm) is around 10°, i.e. between 4 and 5 times the fwhm for the dips of our gold grating samples at $\varphi = 0°$. On the other hand, the fwhm increases with azimuthal angle with a rate which is lower than the sensitivity (S) enhancement, therefore providing an improvement of the figure of merit (FOM = S/fwhm), a relevant tool for considering the whole system sensitivity,[46] as already shown in a previous work.[36]

with SSC 2X and formamide 20%, at a hybridization temperature of 37 °C. Fluorescence microarray hybridization results were collected, and the ratio between the signal on the mutated probe and the one on the wild type probe were calculated, obtaining the discrimination ratios (DR) for each analyzed locus, as shown in Figure 4. These ratios indicate the capacity to discriminate between a perfect and a mismatched target sequence and are necessary to establish a univocal way to genotype unknown samples.

dx.doi.org/10.1021/ac503272y | Anal. Chem. XXXX, XXX, XXX−XXX

Table 3. SPR Shifts Obtained after Hybridization of CFTR Related PCR Products[a]

	screened mutation					
	ΔF508		R1162X		N1303K	
	PCR					
hybridized on	wt PCR	hetero PCR	wt PCR	hetero PCR	wt PCR	hetero PCR
wt probe	0.64° ± 0.06°	0.26° ± 0.06°	0.51° ± 0.06°	0.24° ± 0.07°	0.45° ± 0.07°	0.31° ± 0.08°
mut probe	0.13° ± 0.06°	0.19° ± 0.07°	0.05° ± 0.06°	0.77° ± 0.07°	0.08° ± 0.06°	0.38° ± 0.06°
DR range[b]	0.1−0.2	0.7−3	0.1−0.2	0.7−3	0.1−0.2	0.9−2

[a]Each sample was incubated both on wt and on mut related probe. Values of the shifts are representative of one experiment. [b]DRs are mediated on results of three independent experiments.

Table 4. Hybridization Shift Obtained Incubating the Target PCR Amplicons Alone or Mixed with Interferent Unrelated Genomic DNA Sequences[a]

	target wt/wt DNA								
	ΔF508			R1162X			N1303K		
	probe								
interferent[b]	wt	mut	DR	wt	mut	DR	wt	mut	DR
without	0.56° ± 0.08°	0.13° ± 0.06°	0.23 ± 0.11	0.45° ± 0.06°	0.11° ± 0.07°	0.24 ± 0.16	0.45° ± 0.07°	0.08° ± 0.06°	0.18 ± 0.14
with	0.70° ± 0.07°	0.07° ± 0.06°	0.10 ± 0.09	0.53° ± 0.06°	0.04° ± 0.08°	0.08 ± 0.15	0.45° ± 0.07°	0.12° ± 0.06°	0.27 ± 0.14

[a]Target DNA amplicons derived from homozygous wt/wt samples. [b]Interferent: fragmented genomic DNA (80 ng) and/or unrelated PCR amplicons (300 pg each).

For wt sample (wt/wt), DRs more close to zero are expected for an optimal genotypization indicating that the wt sample is almost completely hybridized on the wt probe. Reported DRs demonstrate that, for all the homozygous wt tested samples, obtained values are suitable for genotyping. In particular, for wt ΔF508 and R1162X, all reported values are included between 0.01 and 0.08. Regarding the N1303K wt sample, the obtained DR is 0.4, relatively higher if compared to the DR rate obtained for the other wt samples, but still able to genotype correctly the sequence.

This can be attributed to the chemico-physical characteristics of N1303K wt and mut probe couple, constrained by the mutation position itself, and by the surrounding nucleotides.

For heterozygous sample (wt/mut), DRs more close to 1 are expected for an optimal genotypization, indicating that the heterozygous sample is equally hybridized on the two probes (wt and mut). Concerning heterozygous samples, for all the tested samples, DRs between 0.9 and 1.3 were achieved: obtained DRs are in line with the expected DR value and are particularly suitable to achieve a precise genotyping of the heterozygous samples.

The optimized condition was used for the hybridization tests on the SPR platform, described in the following section.

SPR Response to PCR Amplified Clinical Samples. Hybridization of CFTR unlabeled PCR products was performed on plasmonic slides. Results are numerically expressed in Table 3 and representative graphs for one analysis are shown in Figure 5. Experiments were performed always in parallel with hybridization on microarray of labeled PCR, as control. Shifts were collected after substrate cleaning, surface biofunctionalization, and sample incubation.

For tested wt samples, a significant shift is recorded after incubation of the sample on the related wt probe (0.45°−0.64°), while no significant signal, i.e., a signal comparable to the measurement error (up to 0.15°), is detected on the mut one (0.05°−0.13°). In the case of heterozygous samples, resonance angle shifts were collected on both relative probes (0.19°−0.77°).

DRs for wild type and heterozygous samples were calculated from the shift ratios. In the case of wt samples DR is included between 0.1 and 0.2 for all the tested samples, underlining genotyping ability of all wt probes in the SPR configuration. Concerning mut probes, DR ranges from 0.7 to 3, underlying that also in this case precise genotypization can be achieved.

SPR Response in the Presence of Interferent DNA. A series of experiments was performed to verify the system genotyping ability in the presence of a more complex sample, resembling the ones routinely used for molecular CF detection, i.e., samples containing several PCR amplified CF related sequences. For this purpose, we used complex samples containing the target sequences and/or both unrelated PCR amplicons or fragmented human genomic DNA. As shown in Table 4, the presence of interferent DNA did not mislead the genotypization of the unknown samples.

The shift signals do not differ between samples, and DR values are all around the threshold value of 0.2 as for the reference noncomplex samples (line without interferent), supporting the correct identification of wild type samples for all of the three investigated alleles.

Further analyses are ongoing to verify the lower limit in sample cellularity in order to reliably detect the presence of mutated sequences in the CFTR gene responsible for CF disease without PCR-mediated amplification.

System Cutoff Evaluation and Test with Blind Samples. After the evaluation of the DRs deriving from all the genotyping experiments performed and summarized in the previous sections, DR cutoffs were established and are reported in Table 5.

A DR cutoff for wt sample genotypization can be set at 0.4: all the obtained DRs below 0.4 univocally genotype a wt sample; vice versa a DR above 0.5 genotypes univocally the presence of a mutant allele. In particular, the presence of a heterozygous sample is characterized by a DR value in the range between 0.5 and 3.0, as verified in our experiments. To validate the genotypization established cutoffs, samples were PCR amplified and analyzed through the SPR platform, in a

dx.doi.org/10.1021/ac503272y | Anal. Chem. XXXX, XXX, XXX−XXX

Table 5. Summary of Genotypization DRs Cutoff Range Obtained Using Fluorescent Technique (a) and SPR Technique (b)

	(a) fluro analysis			(b) SPR analysis	
	DR output results			DR output results	
	wild type	heterozigous		wild type	heterozigous
mut/wt probe signal	<0.4	0.5−1.5	mut/wt probe signal	<0.4	0.5−3.0

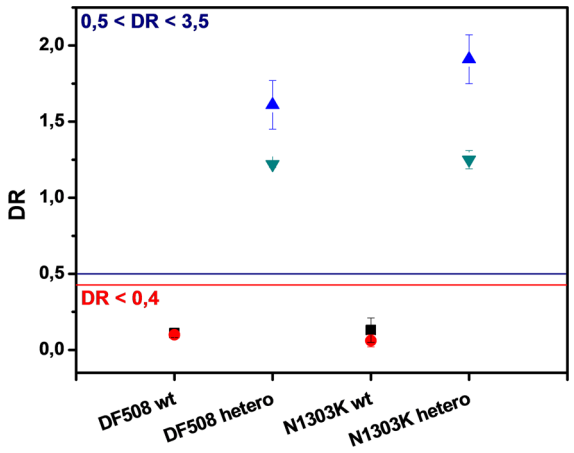

Figure 6. Genotypization of CF samples for the positions related to ΔF508 or N1303K alleles in a blind experiment. The red line represents the DR cutoff for wild type samples, while the blue line points to the lower limit of the DR for heterozygous samples. Red dots and black squares represent replicas of relative wild type samples, while green and blue triangles represent replicas of the relative heterozygous samples.

blind experiment, running a fluorescent microarray experiment as a control. In particular, ΔF508 wild type and heterozygous plus N1303K wild type and heterozygous samples were analyzed in duplicate on the plasmonic gratings. Results are reported in Figure 5, in which shifts are represented as dots on a graph delimited by the DR cutoff lines. For all the analyzed sample's replicas, a correct genotyping was achieved, as shown in the graph (Figure 6). The shifts of wild type samples are below the 0.4 line, while all heterozygous samples present signals above the 0.5 line.

CONCLUSIONS

In this work, probes for CFTR screening were chosen, and their structure was evaluated. A precise and reproducible method for plasmonic gold surface functionalization was optimized for the genotyping of the three most frequent CFTR in the Italian population. Hybridization conditions for correctly genotyping PCR fragments deriving from DNA extracted from clinical samples were properly set using a fluorescent microarray technique. Once optimized, hybridization conditions were used for sample analysis on SPR substrates. Data obtained from plasmonic analysis demonstrated to be fully consistent and homogeneous between replicas, indicating the correct genotypization of the present alleles.

These results clearly showed the possibility of employing azimuthally controlled GC-SPR for the genotypization of CF mutations, and the discrimination between homozygous and heterozygous state could be improved further by finely controlling hybridization parameters to increase the number of the simultaneously detectable mutations. Moreover, the presence of interferent unrelated DNA does not affect the genotyping ability of the optimized SPR system. Further analyses will be performed to establish if the SPR technique could correctly identify mutations also in nonamplified samples, possibly even with the introduction of SPR enhancers. Results shown in the experiments of the present work gave us the starting point for the realization and improvement of a GC-SPR based sensor that could be easily integrated in a diagnostic prototype thanks to the high sensitivity reached by the azimuthally rotated approach and to the system scalability. In fact, even if all the SPR measurements were performed by using a spectroscopic ellipsometer, requiring an expensive readout, the detection system could be easily miniaturized developing a compact prototype as demonstrated in previous works,[47,48] leading to a low cost, label-free mutation screening, with the possibility of integrating the system in a lab-on-a-chip device with temperature and microfluidic control, and suitable also for nonqualified personnel. In addition, using a CCD camera for the plasmonic signal collection, a parallel readout of multiple reactions onto the same substrate could be possible, making the sensing system comparable and complementary to the fluorescence-based detection method. The ability of SPR technique to correctly identify unamplified samples is now under investigation to reduce the test running time.

AUTHOR INFORMATION

Corresponding Author

*E-mail: sonato@iom.cnr.it.

Author Contributions

#These authors contributed equally. All authors have given approval to the final version of the manuscript.

Notes

The authors declare no competing financial interest.

ACKNOWLEDGMENTS

This work has been supported by CARIPARO Foundation and University of Padua: Progetto di Eccellenza SPLENDID: "Surface PLasmonics for Enhanced Nano Detectors and Innovative Devices."

REFERENCES

(1) Rommens, J. M.; Iannuzzi, M. C.; Kerem, B.; Drumm, M. L.; Melmer, G.; Dean, M.; Rozmahel, R.; Cole, J. L.; Kennedy, D. *Science* **1989**, *245*, 1059−1065.

(2) Boat, T., Welsh, M. J.; Beaudet, A. *Cystic Fibrosis*; McGraw-Hill, 1989; The Metabolic Basis of Inherited Disease; pp 2649−2680.

(3) Andersen, D. H. *American Journal of Diseases of Children* **1938**, *56*, 344−399.

(4) Kerem, B. S.; Rommens, J. M.; Buchanan, J. A.; Markiewicz, D.; Cox, T. K.; Chakravarti, A.; Buchwald, M.; Tsui, L. C. *Science* **1989**, *245*, 1073−1080.

(5) Rendine, S.; Calafell, F.; Cappello, N.; Gagliardini, R.; Caramia, G.; Rigillo, N.; Silvetti, M.; Zanda, M.; Miano, A.; Battistini, F.; Marianelli, L.; Taccetti, G.; Diana, M. C.; Romano, L.; Romano, C.; Giunta, A.; Padoan, R.; Pianaroli, A.; Raia, V.; De Ritis, G.; Battistini, A.; Grzincich, G.; Japichino, L.; Pardo, F.; Piazza, A. *Annals of Human Genetics* **1997**, *61*, 411−424.

(6) Picci, L.; Cameran, M.; Marangon, O.; Marzenta, D.; Ferrari, S.; Frigo, A. C.; Scarpa, M. *Journal of Cystic Fibrosis* **2010**, *9*, 29−35.

(7) Castaldo, G.; Rippa, E.; Sebastio, G.; Raia, V.; Ercolini, P.; deRitis, G.; Salvatore, D.; Salvatore, F. *Journal of Medical Genetics* **1996**, *33*, 475−479.

(8) Castaldo, G.; Fuccio, A.; Cazeneuve, C.; Picci, L.; Salvatore, D.; Raia, V.; Scarpa, M.; Goossens, M.; Salvatore, F. *Clinical Chemistry* **1999**, *45*, 957−962.
(9) Chehab F, F.; Wall, J. *Hum. Genet.* **1992**, *89*, 163−168.
(10) Cuppens, H.; Marynen, P.; De Boeck, C.; Cassiman, J.-J. *Genomics* **1993**, *18*, 693−697.
(11) Bradley, L. A.; Johnson, D. A.; Chaparro, C. A.; Robertson, N. H.; Ferrie, R. M. *Genetic Testing* **1998**, *2*, 337−341.
(12) Ferrie, R. M.; Schwarz, M. J.; Robertson, N. H.; Vaudin, S.; Super, M.; Malone, G.; Little, S. *American Journal of Human Genetics* **1992**, *51*, 251−262.
(13) Brinson, E. C.; Adriano, T.; Bloch, W.; Brown, C. L.; Chang, C. C.; Chen, J. G.; Eggerding, F. A.; Grossman, P. D.; Iovannisci, D. A.; Madonik, A. M.; Sherman, D. G.; Tam, R. W.; Winn-Deen, E. S.; Woo, S. L.; Fung, S. *Genetic Testing* **1997**, *1*, 61−68.
(14) Koepf, S. M.; Nguyen, L. Y.; Schreiber, E. *American Journal of Human Genetics* **2002**, *71*, 398−398.
(15) Rommens, J.; Kerem, B. S.; Greer, W.; Chang, P.; Tsui, L. C.; Ray, P. *American Journal of Human Genetics* **1990**, *46*, 395−396.
(16) Grade, K.; Grunewald, I.; Graupner, I.; Behrens, F.; Coutelle, C. *Hum. Genet.* **1994**, *94*, 154−158.
(17) Orita, M.; Iwahana, H.; Kanazawa, H.; Hayashi, K.; Sekiya, T. *Proc. Natl. Acad. Sci. U.S.A.* **1989**, *86*, 2766−2770.
(18) Ferec, C.; Audrezet, M. P.; Mercier, B.; Guillermit, H.; Moullier, P.; Quere, I.; Verlingue, C. *Nature Genetics* **1992**, *1*, 188−191.
(19) Nasef, H.; Beni, V.; O'Sullivan, C. K. *Anal. Bioanal. Chem.* **2010**, *396*, 1423−1432.
(20) Salvado, C. S.; Trounson, A. O.; Cram, D. S. *Reproductive Biomedicine Online* **2004**, *8*, 107−114.
(21) Schrijver, I.; Oitmaa, E.; Metspalu, A.; Gardner, P. *Journal of Molecular Diagnostics* **2005**, *7*, 375−387.
(22) Eaker, S.; Johnson, M.; Jenkins, J.; Bauer, M.; Little, S. *Biosens. Bioelectron.* **2006**, *21*, 933−939.
(23) Clarke, L. A.; Dobson, M.; Galvin, P.; Amaral, M. D. *Pediatric Pulmonology* **2008**, *43*, 283.
(24) Galvin, P.; Clarke, L. A.; Harvey, S.; Amaral, M. D. *Journal of Cystic Fibrosis* **2004**, *3* (Suppl 2), 29−33.
(25) Ubertelli, V.; Bauland, F.; Valat, C.; Josse, C. *ITBM-RBM* **2007**, *28*, 224−229.
(26) Feriotto, G.; Lucci, M.; Bianchi, N.; Mischiati, C.; Gambari, R. *Human Mutation* **1999**, *13*, 390−400.
(27) Feriotto, G.; Ferlini, A.; Ravani, A.; Calzolari, E.; Mischiati, C.; Bianchi, N.; Gambari, R. *Human Mutation* **2001**, *18*, 70−81.
(28) Murphy, D.; Redmond, G. *Anal. Bioanal. Chem.* **2005**, *381*, 1122−1129.
(29) Bassil, N.; Maillart, E.; Canva, M.; Levy, Y.; Millot, M. C.; Pissard, S.; Narwa, W.; Goossens, M. *Sensors and Actuators B Chemical* **2003**, *94*, 313−323.
(30) Mannelli, I.; Courtois, V.; Lecaruyer, P.; Roger, G.; Millot, M. C.; Goossens, M.; Canva, M. *Sensors and Actuators B Chemical* **2006**, *119*, 583−591.
(31) Hottin, J.; Moreau, J.; Spadavecchia, J.; Bellemain, A.; Lecerf, L.; Goossens, M.; Canva, M. *Proceedings - SPIE* **2008**, *6991*, No. 69910Q.
(32) Corradini, R.; Feriotto, G.; Sforza, S.; Marchelli, R.; Gambari, R. *Journal of Molecular Recognition* **2004**, *17*, 76−84.
(33) Feriotto, G.; Corradini, R.; Sforza, S.; Bianchi, N.; Mischiati, C.; Marchelli, R.; Gambari, R. *Laboratory Investigation* **2001**, *81*, 1415−1428.
(34) Li, Y.; Wark, A. W.; Lee, H. J.; Corn, R. M. *Analytical Chemistry* **2006**, *78*, 3158−3164.
(35) Nilsson, P.; Persson, B.; Larsson, A.; Uhlen, M.; Nygren, P. A. *Journal of Molecular Recognition* **1997**, *10*, 7−17.
(36) Romanato, F.; Lee, K. H.; Kang, H. K.; Ruffato, G.; Wong, C. C. *Opt. Express* **2009**, *17*, 12145−12154.
(37) Ruffato, G.; Romanato, F. *Opt. Lett.* **2012**, *37*, 2718−2720.
(38) Sonato, A.; Ruffato, G.; Zacco, G.; Silvestri, D.; Natali, M.; Carli, M.; Giallongo, G.; Granozzi, G.; Morpurgo, M.; Romanato, F. *Sensors and Actuators B - Chemical* **2013**, *181*, 559−566.
(39) Sonato, A.; Silvestri, D.; Ruffato, G.; Zacco, G.; Romanato, F.; Morpurgo, M. *Appl. Surf. Sci.* **2013**, *286*, 22−30.
(40) Buzdin, A. A.; Lukyanov, S. A. *Stem-loop oligonucleotides as hybridization probes and their practical use in molecular biology and biomedicine*; Springer, 2007; Nucleic Acids Hybridization: Modern Applications, pp 85−96.
(41) Broude, N. E. *Trends Biotechnol.* **2002**, *20*, 249−256.
(42) Zielenski, J.; Rozmahel, R.; Bozon, D.; Kerem, B.-s.; Grzelczak, Z.; Riordan, J. R.; Rommens, J.; Tsui, L.-C. *Genomics* **1991**, *10*, 214−228.
(43) Letowski, J.; Brousseau, R.; Masson, L. *J. Microbiol. Methods* **2004**, *57*, 269−278.
(44) Syvanen, A. C. *Nat. Rev. Genet.* **2001**, *2*, 930−942.
(45) Romanato, F.; Lee, K. H.; Ruffato, G.; Wong, C. C. *Appl. Phys. Lett.* **2010**, *96*, 11103−13.
(46) Shalabney, A.; Abdulhalim, I. *Laser & Photonics Reviews* **2011**, *5*, 571−606.
(47) Ruffato, G.; Pasqualotto, E.; Sonato, A.; Zacco, G.; Silvestri, D.; Morpurgo, M. *Sens. Actuators, B* **2013**, *185*, 179−187.
(48) Pasqualotto, E.; Ruffato, G.; Sonato, A.; Zacco, G.; Silvestri, D.; Morpurgo, M.; De Toni, A.; Romanato, F. *Microelectron. Eng.* **2013**, *111*, 348−353.

dx.doi.org/10.1021/ac503272y | *Anal. Chem.* XXXX, XXX, XXX−XXX